Odontology (2023) 111:750–758
https://doi.org/10.1007/s10266-023-00787-z

ORIGINAL ARTICLE

Development and validation of a method for creating incomplete vertical root fracture in extracted teeth

Luiz Carlos de Lima Dias-Junior[1] · Marcio Corrêa[1] · Cleonice da Silveira Teixeira[1] · Diego Leonardo de Souza[1] · Franklin R. Tay[2] · Carlos Estrela[3] · Lucas da Fonseca Roberti Garcia[1] · Eduardo Antunes Bortoluzzi[4]

Received: 16 November 2022 / Accepted: 19 January 2023 / Published online: 28 January 2023

Abstract

The present study reported a method for inducing incomplete root fracture in human extracted teeth for the purpose of evaluating the merits of different diagnostic imaging techniques. Thirty-five single-rooted teeth were inspected under magnification and transillumination to exclude previously fractured teeth. Tooth crowns were removed, and the root canals were prepared up to the ProTaper Next X4 (40.06) file. Each root was lined with wax and embedded in a polystyrene resin block. The setup was attached to a universal testing machine for pressing a customized conical wedge (diameter at tip: 0.6 mm; taper: 0.2 mm/mm) into the instrumented canal with a 2 kN load at 5 mm/min. The machine was programmed to stop after a sudden 10% drop in loading force. Each specimen was removed from the resin block and inspected under × 20 magnification and transillumination to identify the fracture characteristics (pattern, surfaces and root-third affected). The gap width of each specimen was measured at different locations along the fracture line. The protocol induced incomplete vertical root fractures in all specimens. Fracture widths were < 100 µm in all specimens (mean gap width: 34.9 µm). The proposed methodology was successful in inducing incomplete vertical root fractures with characteristics that resemble the clinical presentation of these conditions. The method is easy to execute, highly reproducible and helps to minimize bias in laboratory studies that aims to mimic vertical root fractures.

Keywords Cone-beam computed tomography · Diagnosis · Endodontics · Fracture width · Vertical root fracture

Introduction

Cracks and fractures are often found in teeth with extensive restorations [1]. They may occur immediately upon completion of the restoration or after a long period or intraoral function [1]. Horizontal root fracture is highly associated with dental trauma [1]. An impact with substantial kinetic energy causes immediate horizontal fracture of the root structure [1]. Conversely, vertical root fracture (VRF) may be caused by trauma or fatigue, with persistent occlusal forces slowly causing rupture of the tooth substrate [1].

The etiology of VRF is multifactorial [2]. These fractures are often associated with excessive occlusal forces, parafunctional habits, dental trauma or after root canal treatment [3]. Iatrogenic factors during root canal treatment include excessive root canal enlargement, exaggerated forces during lateral or vertical compaction of root canal filling or insertion of intraradicular screw posts [4].

Vertical root fractures are longitudinally oriented fractures of the root [1]. They represent ~ 2–5% of all dental fractures [3] and are present in 3.7–13.4% of root-treated teeth [5]. Vertical root fractures occur more frequently in older patients and represent 7.7–32.1% of all causes of tooth extraction [6]. In root-treated teeth, VRFs are the third most common reason for extraction [5]. The communication between the root canal and the periodontium created by a

✉ Lucas da Fonseca Roberti Garcia
drlucas.garcia@gmail.com

1 Department of Dentistry-Endodontics Division, Health Sciences Center, Federal University of Santa Catarina, Campus Reitor João David Ferreira Lima, Florianópolis, Santa Catarina, Brazil

2 Department of Endodontics, The Dental College of Georgia, Augusta University, Augusta, GA, USA

3 Department of Endodontics, School of Dentistry, Federal University of Goiás, Goiânia, Brazil

4 Department of Diagnosis & Oral Health, Division of Endodontics, School of Dentistry, University of Louisville, Louisville, KY, USA

VRF creates a pathway for bacterial contamination, which results in rapid alveolar bone loss. Prompt and accurate diagnosis of VRF is required to prevent additional damage to the alveolar bone by removing the cause of inflammation and the source of contamination [3].

The diagnosis of VRF is a colossal challenge to dental clinicians [2]. Clinical signs and symptoms are often non-specific, such as the presence of deep osseous defects or sinus tracts. There is also a lack of pathognomonic signs and symptoms [3]. A robust diagnostic strategy needs to involve a patient's dental history, clinical signs and symptoms, as well as radiographic imaging [1]. During the initial stage of VRFs, the clinical signs are similar to those of failed root canal therapy, periodontal disease or even endodontic-periodontal complications [7]. Hence, it is essential to differentiate VRF from other clinical problems. Imaging plays an important role in the differential diagnosis of the clinical problem.

Cone-beam computed tomography (CBCT) has been used for attempted detection of VRFs in unfilled roots [7–10]. However, VRF diagnosis using CBCT is severely hindered in the presence of root canal fillings or metal posts [7–10]. These high-density materials create beam-hardening artifacts which resemble fracture lines [7–10]. Diagnostic accuracy is compromised in incomplete VRFs even with the use of high-resolution CBCT [7–10]. This is attributed to minimal separation of the fractured root fragments that is typically found in these cases [11]. Because the prognosis of VRF is poor, the only possible approach in most cases is tooth extraction [10].

Countless efforts have been made to develop tools that improve the diagnostic accuracy of CBCT imaging in detecting VRFs, particularly in the presence of root canal fillings or metallic posts. Artifact reduction algorithms [12–14] and filters [7, 15, 16] have been evaluated, associated with acquisition parameters such as resolution [7, 15, 17] and field of view [14, 17]. Nevertheless, definitive diagnosis of VRFs, especially incomplete VRFs, often requires invasive exploratory surgery [6, 18]. Studies that evaluate the diagnosis of incomplete VRFs are urgently needed to improve diagnostic accuracy and reduce the need of invasive procedures.

Diagnostic research on VRF is challenging because its identification depends on different aspects, such as fracture width [11, 19–21], direction (buccolingual or mesiodistal) [7] and the tooth position in the field of view (central or peripheral) [14]. Previous studies artificially induced complete VRFs and bonded the fragments back to simulate incomplete root fractures [9, 15]. This technical procedure does not simulate the clinical features of VRF in terms of fracture width and fragment position [11]. Moreover, fractured teeth with more than two fragments or fracture patterns that do not permit repositioning are usually discarded, causing unnecessary loss of specimens [8, 10, 12, 22].

There is limited reproducibility of the methodologies used to induce artificial incomplete VRF in extracted human teeth. Towards this objective, the development of a highly reproducible and evidence-based laboratory model able to identify the presence of incomplete VRFs is crucial. Accordingly, the purpose of the present in vitro study was to develop and to validate a deep learning method for creating incomplete VRF in single-rooted human teeth.

Material and methods

Sample selection

The present in vitro study was conducted in accordance with the Preferred Reporting Items for Laboratory studies in Endodontology (PRILE) 2021 guidelines [23]. The study proposal was approved by the institutional Ethics Committee (Protocol n. 4.444.914/2020). Freshly extracted human permanent teeth were selected with consent received by the donors for the use of the unidentified teeth for benchtop research. Single-rooted teeth were used to avoid anatomic differences that might complicate the analysis and create bias. The teeth were inspected under stereomicroscope (Stereo Discovery V12; Carl Zeiss, Oberkochen, Germany) at × 20 magnification and transillumination. Teeth with open apices, root curvatures, supernumerary roots, obliterated canals, pulp calcifications, internal/external resorption, root canal fillings, cavities or pre-existing cracks/fractures were excluded from the final sample. Periapical radiographs were taken and examined by a previously trained radiologist to validate the specimen selection.

Specimen preparation

The selected teeth were hand-scaled to remove soft tissue and calculus. The cleaned teeth were disinfected with 2% glutaraldehyde for two hours and kept hydrated until fractures were induced. The tooth crowns were sectioned at the cementoenamel junction with a double-sided diamond saw (Buehler Ltd., Lake Bluff, IL, USA) coupled to a metallographic-cutter (Isomet 1000; Buehler Ltd.) under copious water cooling. A size 10 K-file (Dentsply Maillefer, Ballaigues, Switzerland) was placed in the canal until it was visible at the apical foramen. The working length was determined by subtracting 1 mm from this measurement.

The root canals were prepared with nickel-titanium rotary instruments (ProTaper Next; Dentsply Sirona, Bensheim, Germany). To standardize the apical portion up to a size 40/0.06 instrument, the instruments X1 (17/0.04), X2 (25/0.06), X3 (30/0.07) and X4 (40/0.06) were sequentially used. Each instrument was coupled to a 6:1 contra-angle device powered by an electric motor (X-Smart Plus;

Dentsply Sirona), driven in rotary motion (400 rpm; 2 Ncm) with light apical pressure. Gentle back-and-forth motions were used until the working length reaching and each instrument was capable of rotating freely within the root canal. Foraminal patency was maintained with a size 10 K-file (Dentsply Maillefer). The root canals were irrigated with 2 mL of 2.5% sodium hypochlorite solution (Rio Química, São José do Rio Preto, SP, Brazil) at each instrument change. The irrigating solution was delivered within the root canals with a 5 mL syringe (Ultradent, Salt Lake City, UT, USA) and a 30-gauge needle (Endo-Eze; Ultradent) with back-and-forth movements. After completion of the chemical–mechanical preparation, the root canals were irrigated with 5 mL of 2.5% sodium hypochlorite solution and dried with absorbent paper cones (Dentsply Maillefer).

Incomplete VRF induction

Each tooth root was lined with a 1-mm-thick layer of wax and temporarily fixed in polystyrene resin (ComFibras, Florianopolis, SC, Brazil) to 3 mm from the CEJ, using a cylindrical mold (19 mm in diameter × 24 mm in height). Fractures were induced with a universal testing machine (Instron Corp., Canton, MA, USA). The fractures were mechanically created by applying a customized metallic wedge apically at the root canal. The tapered metal wedge was placed inside the root canal. The testing machine was set to apply a maximum load of 2 kN. The universal testing machine was programed to stop automatically when 10% force reduction was recorded. This force was strong enough to create root dentin fracture without fragment separation, producing an incomplete VRF [24] (Fig. 1).

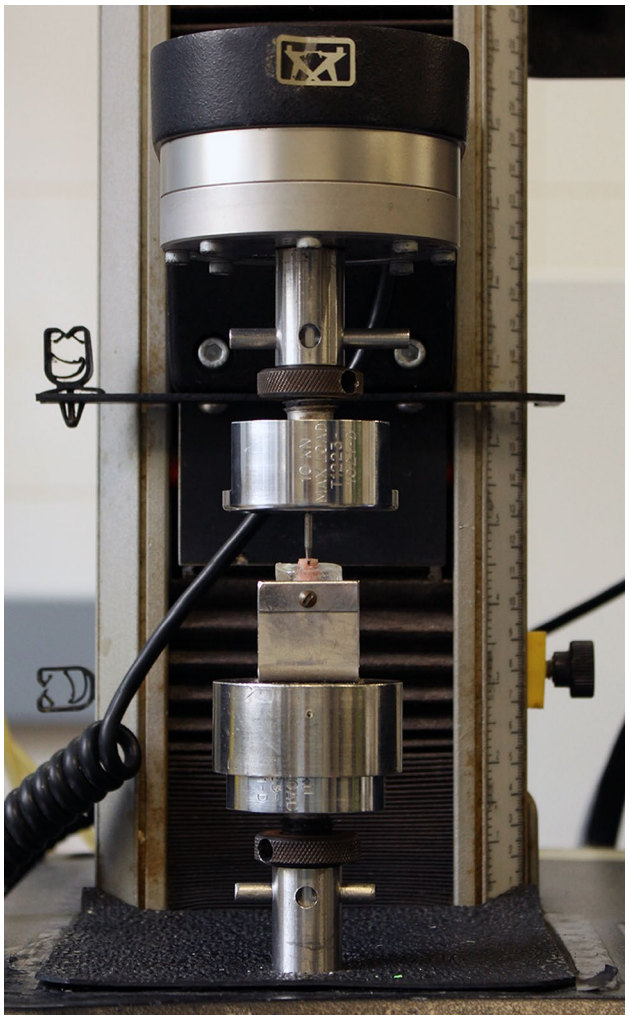

Fig. 1 Experimental setup for inducing incomplete *VRF* a universal test machine with the specimen temporarily fixed in an acrylic resin block. Each specimen was positioned in a fixed platform with the metal conical wedge inside the root canal. A flat base was adapted to the top of the testing machine to gradually force the wedge into the root canal

Pilot study

A pilot study was conducted to identify the most appropriate characteristics for creating incomplete VRFs. The following wedges were tested in the pilot study: 40.3 (diameter at tip = 0.4 mm; taper = 0.3 mm/mm); 60.2 (diameter at tip = 0.6 mm; taper = 0.2 mm/mm) and 60.05 (diameter at tip = 0.6 mm; taper = 0.05 mm/mm). In addition, two crosshead speeds were tested: 1 mm/min and 5 mm/min. Thirty specimens were used in the pilot study, with six groups of five teeth each for testing the customized wedges and crosshead speeds.

Each specimen was removed from the resin block immediately after fracture to verify the presence of incomplete VRF. Examination was performed under stereomicroscope (Stereo Discovery V12; Carl Zeiss) at × 20 magnification and transillumination. The success rate of the experimental groups from the pilot study was compared using the Fisher Exact test (SPSS Statistics, Version 25.0; IBM Corp., IBM Armonk, NY, USA). Statistical significance was set at $\alpha = 0.05$.

Success rate

The most appropriate protocol was further analyzed for its success rate in creating incomplete VRNs to ensure the reproducibility of the protocol. Sample size was calculated using data from the pilot study. A priori power analysis

indicated that a total of 35 teeth would be required for 5% error margin and 95% confidence level. Using the protocol selected from the pilot study, 35 additional teeth were subjected to the VRF induction.

After fracture, the 35 specimens were re-inspected under stereomicroscope (Stereo Discovery V12; Carl Zeiss) at × 20 magnification and transillumination. Additional verification was performed using 1% methylene blue dye to highlight the pathway of each fracture (Fig. 2). The fracture pattern (complete or incomplete fracture) affected root surface (buccal, lingual, mesial, distal or combination), extension (root-thirds involved: cervical, middle or apical) and the fracture origin (cervical or apical) were recorded.

Fracture width

Fracture width was determined by a previously calibrated and trained examiner, using a stereomicroscope video-based system (Stereo Discovery V12; Carl Zeiss, Oberkochen, Germany) installed with the AxioVision v. 4.8.3 software (Carl Zeiss). A plastic transparent ruler was positioned on top of the cervical aspect of each specimen as a measuring scale. The distance between fragments was measured at three points: P1—as close as possible to the root canal; P2—as close as possible to the external root surface; and P3—intermediate point between P1 and P2 (Fig. 3). This was repeated for both fracture lines of each specimen. The values from P1, P2, and P3 of both fracture lines were used to calculate the mean fracture width for each specimen.

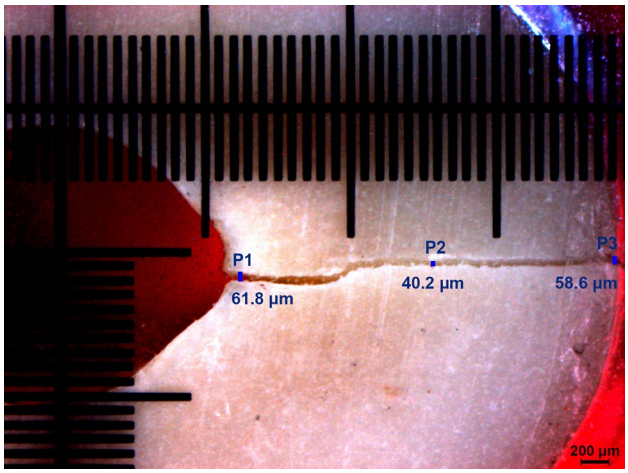

Fig. 3 Representative stereomicroscopic image of a narrow incomplete VRF with gap width measurements at locations P1, P2 and P3 (see text for detailed descriptions of these locations)

Results

Pilot study

There was a statistically significant difference among the tested protocols of the pilot study ($P < 0.05$). The success rate of the protocol that used a 60.2 wedge at 5 mm/min was significantly higher than the other protocols ($P < 0.05$).

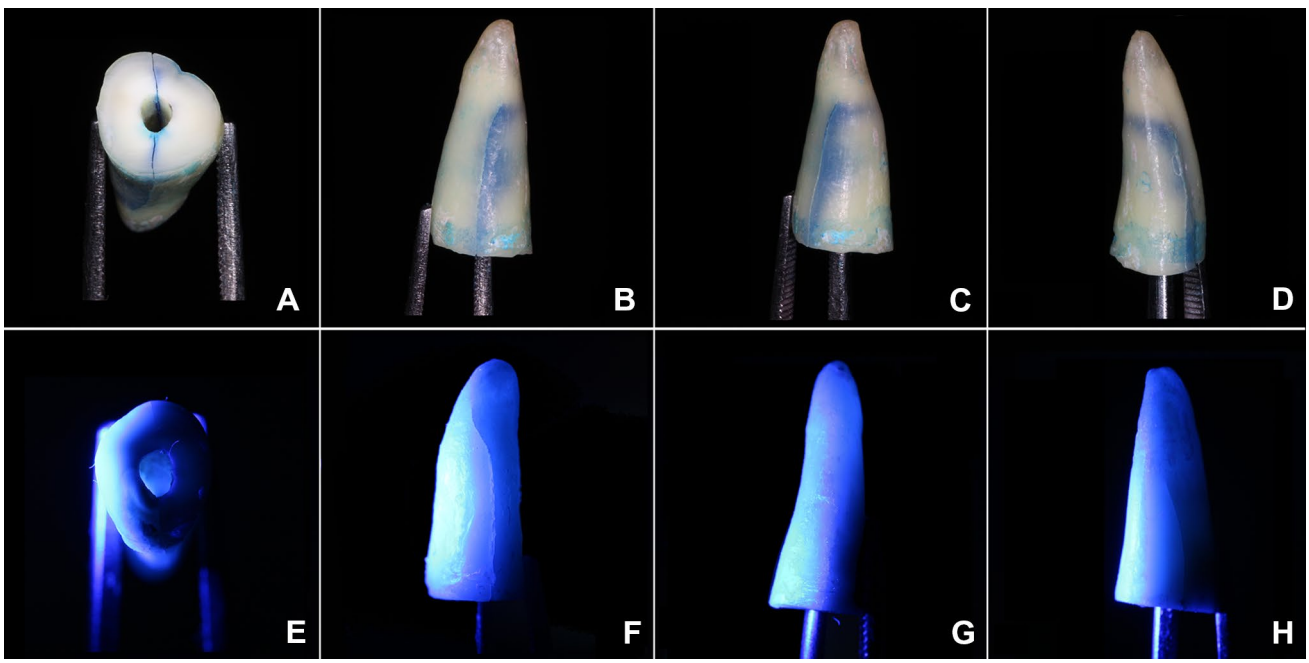

Fig. 2 Inspection via application of 1% methylene blue (**A**, **B**, **C** and **D**), and light-emitting diode transillumination (**E**, **F**, **G** and **H**) for identification and characterization of incomplete VRFs

This protocol successfully induced incomplete VRFs in all 5 specimens. When the 60.2 wedge was used at 1 mm/min, two specimens were lost because it chipped the coronal third, creating an unrealistic fracture that was not vertically oriented. The protocols using the 40.3 wedge also chipped the coronal third in three of the specimens, regardless of the crosshead speed.

The 60.05 wedge created catastrophic failure with multiple fragments at the apical third of three specimens when the crosshead speed of 1 mm/min was employed. Likewise, the 60.05 wedge created similar catastrophic failure in two specimens when the crosshead speed of 5 mm/min was employed. In addition, one specimen from each group was lost because of the generation of a complete VRF.

Final success rate

The overall success rate of the protocol using 60.2 wedge at 5 mm/min was 100%. Incomplete root fracture was obtained for all 35 specimens. There was no loss of specimens that was attributed to complex root fractures or complete separation of fragments. Regarding the root thirds that were affected by the fracture line, in 8 specimens the fracture was limited to the cervical root third, 20 specimens presented fractures at the cervical and middle root thirds, and in 7 specimens the fracture extended to the apical root third (Fig. 4A). The mean fracture width was 34.9 µm (20.4–86.3 µm) (Fig. 4B). Table 1 summarizes the fracture characteristics of each specimen and the respective mean fracture width.

Discussion

Incomplete VRFs, also known as hairline fractures, are manifested by minimal fragment separation. These fractures are not easily detected by periapical radiographs [11, 22] and are less likely to be associated with abrupt increases in periodontal pocket depth and the presence of sinus tracts [22]. CBCT is insensitive and has low specificity in diagnosing hairline fracture [19, 22], even for teeth with unfilled root canals [11, 20].

Although the diagnosis of VRF has been extensively investigated using in vitro studies, the methods used so far to induce root fractures are heterogeneous and often poorly described. In a method reported for inducing complete VRFs in canine teeth, a conical wedge was placed inside the root canal and tapped with a hammer in the apical direction [25]. This method had been utilized by several studies for artificially producing incomplete VRF [8, 13, 19, 20]. Other studies created artificial incomplete VRFs by splitting teeth directly with a chisel and hammer [7, 9]. Some studies induced fractures by placing a pin inside the root canal and turning with a screwdriver [14] or wrench [12]. Another study applied mechanical force directly to the roots with a hammer placed on a soft rubber foundation [15]. These methods suffer from serious reproducibility problems. Information is lacking on the characteristics of the wedges [8, 10, 13, 19–21], pins [14, 15] or chisels [7, 9, 21], as well as the magnitude and direction of load applied to the teeth [7–10, 13, 15, 19–21]. Because these variables are difficult to control, it is unlikely that these methods can be accurately replicated.

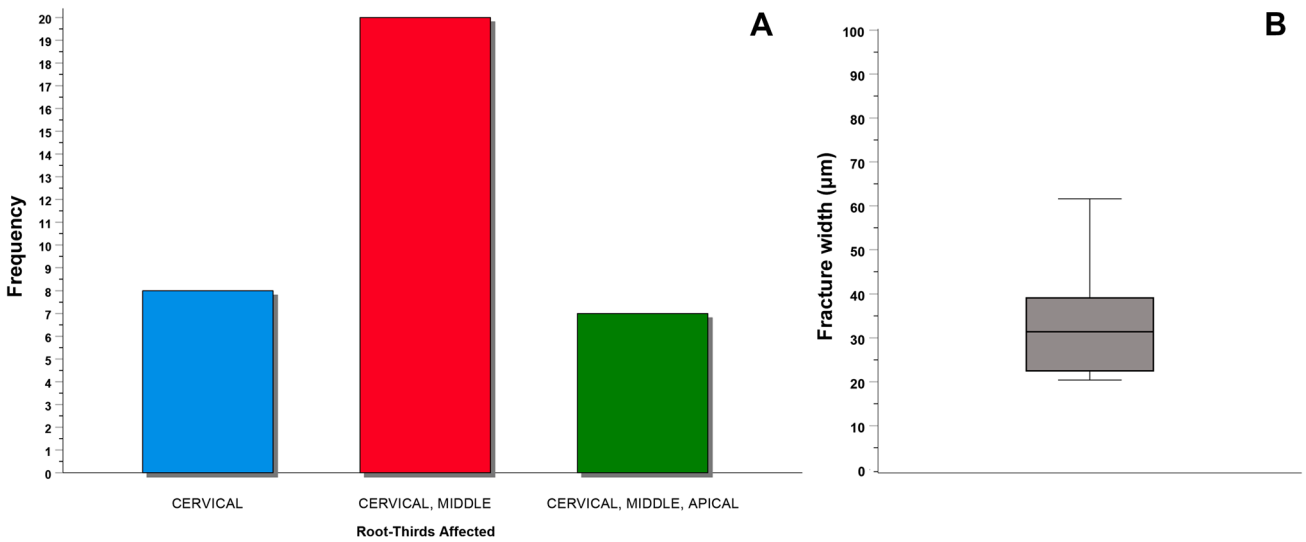

Fig. 4 Frequency of root thirds affected by the fracture lines (**A**). Box-plot of the mean fracture width (µm) (**B**)

Table 1 Vertical root fracture characteristics, including tooth type, fracture pattern and origin, surfaces and root-thirds affected by the fractures, and mean fracture width of the experimental protocol (60.2 wedge at 5 mm/min)

Sample	Tooth	Pattern	Surfaces affected	Root-thirds affected	Fracture origin	Mean fracture width (μm)
1	11	Incomplete	B, L	Cervical, middle	Cervical	50.7
2	22	Incomplete	M, D	Cervical, middle	Cervical	38.1
3	12	Incomplete	B, L	Cervical	Cervical	22.2
4	35	Incomplete	B, L	Cervical, middle, apical	Cervical	20.4
5	11	Incomplete	MB, DL	Cervical, middle, apical	Cervical	86.3
6	12	Incomplete	B, L	Cervical, middle, apical	Cervical	38.4
7	44	Incomplete	B, DL	Cervical, middle	Cervical	57.2
8	35	Incomplete	M, D	Cervical, middle	Cervical	39.8
9	22	Incomplete	B, L	Cervical	Cervical	31.5
10	15	Incomplete	MB, ML	Cervical, middle	Cervical	32.5
11	21	Incomplete	B, L	Cervical, middle, apical	Cervical	37.2
12	45	Incomplete	DB, L	Cervical	Cervical	32.1
13	12	Incomplete	B, L	Cervical, middle	Cervical	51.9
14	21	Incomplete	B, L	Cervical, middle	Cervical	61.6
15	25	Incomplete	B, L	Cervical, middle, apical	Cervical	65.9
16	21	Incomplete	MB, DL	Cervical, middle	Cervical	28.5
17	45	Incomplete	M, D	Cervical, middle	Cervical	22.4
18	11	Incomplete	M, D	Cervical	Cervical	21.9
19	21	Incomplete	MB, ML	Cervical	Cervical	46.2
20	12	Incomplete	DB, L	Cervical, middle	Cervical	28.2
21	12	Incomplete	MB, DL	Cervical, middle	Cervical	24.5
22	35	Incomplete	B, L	Cervical, middle, apical	Cervical	49.3
23	21	Incomplete	MB, DL	Cervical, middle	Cervical	31.4
24	44	Incomplete	ML, D	Cervical, middle	Cervical	20.8
25	12	Incomplete	M, D	Cervical, middle, apical	Cervical	34.8
26	21	Incomplete	DB, ML	Cervical, middle	Cervical	21.3
27	15	Incomplete	M, D	Cervical	Cervical	25.1
28	21	Incomplete	B, D	Cervical, middle	Cervical	23.2
29	34	Incomplete	MB, ML	Cervical, middle	Cervical	22.4
30	35	Incomplete	M, DB	Cervical, middle	Cervical	21.4
31	11	Incomplete	M, D	Cervical, middle	Cervical	30.2
32	12	Incomplete	M, MB	Cervical, middle	Cervical	22.6
33	15	Incomplete	DB, ML	Cervical	Cervical	21.5
34	34	Incomplete	B, D	Cervical	Cervical	34.4
35	11	Incomplete	MB, DL	Cervical, middle	Cervical	25.3

B buccal, *L* lingual, *M* mesial, *D* distal, *MB* mesiobuccal, *ML* mesiolingual, *DB* distobuccal, *DL* distolingual

Although some studies employed universal testing machines to create incomplete VRFs [11, 16, 17, 22], the settings varied in terms of forces and crosshead speeds. The crosshead speed that was most commonly used was 1 mm/min [11, 16, 22]. Regarding the characteristics of the wedges or conical tips applied to the root canals, there is a general lack of information on their diameters and tapers [16, 17]. However, the characteristics of the wedges or pins also affected the technique. A thin sewing needle was used to induce incomplete VRF and a large needle was used to induce complete VRF with a universal testing machine [22]. In the present work, a pilot study was performed using different types of wedges and pins with different diameters and tapers. A common observation in the pilot study was that the teeth usually chipped at the cervical region with the use of low crosshead speeds. The most consistent setting to induce incomplete VRF was identified to be 5 mm/min. The use of a highly tapered pin (40.3) also caused chipping of the cervical region. In contrast, wedges with lower tapers usually created catastrophic root dentin failure at the apical region (60.05). A conical wedge with 0.6 mm diameter at the tip and 0.2 mm/mm taper was ultimately chosen. This

instrument enabled the authors to create incomplete VRF reliably.

Previous studies [11, 22, 26] programmed the universal testing machine to automatically stop applying loading force upon a sudden drop in force of 20% or more. This method was modified in the present work by setting the threshold to 10%. In this manner, it is possible to check the propagation of the fracture line after the machine stopped; further loading force may be applied if required. For creating incomplete VRF, it was necessary to create a customized support base to fix the specimen at the platform of the universal testing machine. This support base prevented further spontaneous propagation of the fracture and prevented the tooth from splitting into two fragments (i.e., complete VRF).

The diagnostic accuracy of CBCT depends on the width of the VRF [11, 19–21]. It has been reported [22] that an incomplete VRF which is less than 150 µm wide is impossible to create using a chisel and hammer or tapping a conical wedge into the root canal. According to those authors, the widths of the fractures obtained using these methods were over 200 µm, which approximate complete VRF more than incomplete VRF [11, 22]. The present study attempted to establish a highly reproducible method to induce incomplete VRFs that simulate clinical scenarios. Therefore, it was imperative to control the fracture width. Clinically, incomplete VRFs usually have minimal fragment separation, with an average gap size of 53.5 µm [11]. The method reported in the present study successfully reproduced the width range of in vivo incomplete VRFs [22], with a mean gap width of 34.9 µm.

Clinically, the width of VRFs ranges from 60 to 770 µm [27]. Incomplete VRFs have gap widths between 30 and 110 µm[11, 22], while the gap widths of complete VRFs are usually over 200 µm [22]. After induction of complete VRFs, some studies bonded the fragments together to simulate incomplete VRFs [8, 10, 15, 17]. Although most of the published studies did not report the fracture width, it is unlikely that investigations with bonded fragments generated fractures with gap widths that are smaller than 200 µm [21]. Thus, previous studies might have created artificial VRFs that are unrealistic in simulating clinical incomplete VRFs [8, 10, 13, 15, 17, 21].

The present study induced root fractures using a quasi-static model. In this model, the wedge was progressively introduced into the root canal, with increased applied force, until the fracture occurs. Conversely, a dynamic model based on fatigue loading has been used to evaluate the fracture resistance of endodontically treated teeth [28]. It is likely that most vertical root fractures occur after repetitive occlusal loading due to fatigue, rather than a single episode of high occlusal stress. However, it is impossible to clinically differentiate these two conditions in the diagnosis of VRFs. The use of fatigue loading to induce VRFs might impair the method's reproducibility in consistently producing incomplete VRFs.

With respect to reproducibility, one may argue that differences in the root surface morphology, the root-third in which VRF occurs, as well as the fracture width, may invalidate the proposed method. However, the progress of fracture through dentin is dependent upon tooth structure factors such as dentin volume, root canal shape and the presence of sclerotic dentin [29]. These features are impossible to be standardized. The fracture width varied from 20.4 to 86.3 µm. Considering the microscopical scale of incomplete VRFs, this difference is clinically insignificant. Moreover, the clinical aspect of VRFs is highly variable, producing identical VRFs would have no practical value for in vitro diagnostic studies. The present manuscript does not deliver direct new evidence. However, it offers support for further diagnostic investigations by providing a reliable method to artificially create incomplete VRFs. The current method has been demonstrated in different single-rooted teeth (i.e., maxillary incisors and maxillary/mandibular premolars). Specimen selection criteria did not include the anatomical diameter of the root canals nor the root shape (i.e., round, oval, long oval). This is because over-restricting the criteria for standardization of tooth specimens will hinder the reproducibility of the method employed. The objective here was to develop a method that can be replicated using single-rooted teeth.

Notwithstanding the numerous efforts to calibrate operators and standardize fracture methods, problems of specimen wastage have been reported [8, 12, 13, 15, 22]. Specimen loss due to fracture with more than two fragments occurs in 13.3–25% of the specimens [8, 22]. Because of the lower reproducibility of the fracture methods, it has been reported that 6–10 specimens must be used in pilot experiments to determine the load required to induce root fracture [13, 15]. In comparison, there was no specimen loss in the present study, with a 100% success rate in creating incomplete VRF. Although most fractures occurred at the buccal and lingual surfaces and propagated across the cervical and middle root-thirds, the methodology presented created different types of incomplete VRF similar to the clinical manifestations of this condition. Because fracture induction was performed in a controlled manner, it is possible to apply additional loading forces to the specimens, after examination of the incomplete VRFs, to obtain complete VRFs.

Conclusions

The protocol reported in the present study bridged a gap in the current literature, on the availability of a reliable method to create laboratory-induced incomplete VRFs that simulate the clinical characteristics of these conditions. The method

had high efficacy, producing incomplete VRFs in all tested specimens.

Acknowledgements The authors would like to thank the "Coordenação de Aperfeiçoamento de Pessoal de Nível Superior (CAPES)" for the financial assistance to carry out this research.

Author contributions LdeL: conceptualization, methodology, investigation, writing—original draft; MC: conceptualization, methodology; CdaST: methodology, investigation, writing—review & editing; DLdeS: methodology, investigation, writing—review & editing; FRT: validation, formal analysis; CE: resources, data curation; LdaFRG: conceptualization, writing—review & editing, project administration, funding acquisition, supervision; EAB: conceptualization, writing—review & editing, project administration, funding acquisition.

Data availability The datasets generated during and/or analysed during the current study are available in the UFSC Library repository (https://repositorio.ufsc.br/).

Declarations

Conflict of interest The authors declare that they have no known competing financial interests or personal relationships that could have appeared to influence the work reported in this paper.

Ethical approval All procedures performed in studies involving human participants were in accordance with the ethical standards of the institutional and/or national research committee and with the 1964 Helsinki Declaration and its later amendments or comparable ethical standards. The study was approved by the thics Committee of the Federal University of Santa Catarina—UFSC—(No. 4.444.914/2020).

References

1. Rivera EM, Walton RE. Longitudinal tooth cracks and fractures: an update and review. Endod Top. 2015;33(1):14–42.
2. Garcia-Guerrero C, Parra-Junco C, Quijano-Guauque S, Molano N, Pineda GA, Marin-Zuluaga DJ. Vertical root fractures in endodontically-treated teeth: a retrospective analysis of possible risk factors. J Investig Clin Dent. 2018. https://doi.org/10.1111/jicd.12273.
3. Cohen S, Blanco L, Berman L. Vertical root fractures: clinical and radiographic diagnosis. J Am Dent Assoc. 2003;134(4):434–41.
4. Fuss Z, Lustig J, Katz A, Tamse A. An evaluation of endodontically treated vertical root fractured teeth: impact of operative procedures. J Endod. 2001;27(1):46–8.
5. Toure B, Faye B, Kane AW, Lo CM, Niang B, Boucher Y. Analysis of reasons for extraction of endodontically treated teeth: a prospective study. J Endod. 2011;37(11):1512–5.
6. Chen SC, Chueh LH, Hsiao CK, Wu HP, Chiang CP. First untoward events and reasons for tooth extraction after nonsurgical endodontic treatment in Taiwan. J Endod. 2008;34(6):671–4.
7. De Martin ESD, Campos CN, Pires Carvalho AC, Devito KL. Diagnosis of mesiodistal vertical root fractures in teeth with metal posts: influence of applying filters in cone-beam computed tomography images at different resolutions. J Endod. 2018;44(3):470–4.
8. Dutra KL, Pacheco-Pereira C, Bortoluzzi EA, Flores-Mir C, Lagravere MO, Correa M. Influence of intracanal materials in vertical root fracture pathway detection with cone-beam computed tomography. J Endod. 2017;43(7):1170–5.
9. Hassan B, Metska ME, Ozok AR, van der Stelt P, Wesselink PR. Detection of vertical root fractures in endodontically treated teeth by a cone beam computed tomography scan. J Endod. 2009;35(5):719–22.
10. Melo SL, Bortoluzzi EA, Abreu-Junior M, Correa LR, Correa M. Diagnostic ability of a cone-beam computed tomography scan to assess longitudinal root fractures in prosthetically treated teeth. J Endod. 2010;36(11):1879–82.
11. Brady E, Mannocci F, Brown J, Wilson R, Patel S. A comparison of cone beam computed tomography and periapical radiography for the detection of vertical root fractures in nonendodontically treated teeth. Int Endod J. 2014. https://doi.org/10.1111/iej.12209.
12. Dalili Kajan Z, Taramsari M, Khosravi Fard N, Khaksari F, Moghasem HF. The Efficacy of metal artifact reduction mode in cone-beam computed tomography images on diagnostic accuracy of root fractures in teeth with intracanal posts. Iranian Endodontic J. 2018;13(1):47–53.
13. de Rezende Barbosa GL, Sousa Melo SL, Alencar PN, Nascimento MC, Almeida SM. Performance of an artefact reduction algorithm in the diagnosis of in vitro vertical root fracture in four different root filling conditions on CBCT images. Int Endod J. 2016;49(5):500–8.
14. Nikbin A, Dalili Kajan Z, Taramsari M, Khosravifard N. Effect of object position in the field of view and application of a metal artifact reduction algorithm on the detection of vertical root fractures on cone-beam computed tomography scans: an in vitro study. Imaging Sci Dent. 2018;48(4):245–54.
15. Wenzel A, Haiter-Neto F, Frydenberg M, Kirkevang LL. Variable-resolution cone-beam computerized tomography with enhancement filtration compared with intraoral photostimulable phosphor radiography in detection of transverse root fractures in an in vitro model. Oral Surg Oral Med Oral Pathol Oral Radiol Endod. 2009;108(6):939–45.
16. Gaeta-Araujo H, Nascimento EHL, Oliveira-Santos N, Queiroz PM, Oliveira ML, Freitas DQ, et al. Effect of digital enhancement on the radiographic assessment of vertical root fractures in the presence of different intracanal materials: an in vitro study. Clin Oral Investig. 2021;25(1):195–202.
17. Queiroz PM, Santaella GM, Capelozza ALA, Rosalen PL, Freitas DQ, Haiter-Neto F. Zoom reconstruction tool: evaluation of image quality and influence on the diagnosis of root fracture. J Endod. 2018;44(4):621–5.
18. Quintero-Alvarez M, Bolanos-Alzate LM, Villa-Machado PA, Restrepo-Restrepo FA, Tobon-Arroyave SI. In vivo detection of vertical root fractures in endodontically treated teeth: accuracy of cone-beam computed tomography and assessment of potential predictor variables. J Clin Exp Dent. 2021;13(2):e119–31.
19. Byakova SF, Novozhilova NE, Makeeva IM, Grachev VI, Kasatkina IV. The detection of vertical root fractures in post-core restored teeth with cone-beam CT: in vivo and ex vivo. Dentomaxillofac Radiol. 2019;48(6):20180327.
20. Makeeva IM, Byakova SF, Novozhilova NE, Adzhieva EK, Golubeva GI, Grachev VI, et al. Detection of artificially induced vertical root fractures of different widths by cone beam computed tomography in vitro and in vivo. Int Endod J. 2016;49(10):980–9.
21. Ozer SY. Detection of vertical root fractures of different thicknesses in endodontically enlarged teeth by cone beam computed tomography versus digital radiography. J Endod. 2010;36(7):1245–9.
22. Patel S, Brady E, Wilson R, Brown J, Mannocci F. The detection of vertical root fractures in root filled teeth with periapical radiographs and CBCT scans. Int Endod J. 2013;46(12):1140–52.
23. Nagendrababu V, Murray PE, Ordinola-Zapata R, Peters OA, Rocas IN, Siqueira JF Jr, et al. PRILE 2021 guidelines for reporting laboratory studies in endodontology: a consensus-based development. Int Endod J. 2021;54(9):1482–90.

24. Fayad MI, Ashkenaz PJ, Johnson BR. Different representations of vertical root fractures detected by cone-beam volumetric tomography: a case series report. J Endod. 2012;38(10):1435–42.
25. Monaghan P, Bajalcaliev JG, Kaminski EJ, Lautenschlager EP. A method for producing experimental simple vertical root fractures in dog teeth. J Endod. 1993;19(10):512–5.
26. Fox A, Basrani B, Lam EWN. The performance of a zirconium-based root filling material with artifact reduction properties in the detection of artificially induced root fractures using cone-beam computed tomographic imaging. J Endod. 2018;44(5):828–33.
27. Chavda R, Mannocci F, Andiappan M, Patel S. Comparing the in vivo diagnostic accuracy of digital periapical radiography with cone-beam computed tomography for the detection of vertical root fracture. J Endodontics. 2014;40(10):1524–9.
28. Ambica K, Mahendran K, Talwar S, Verma M, Padmini G, Periasamy R. Comparative evaluation of fracture resistance under static and fatigue loading of endodontically treated teeth restored with carbon fiber posts, glass fiber posts, and an experimental dentin post system: an in vitro study. J Endod. 2013;39(1):96–100.
29. Sodvadiya UB, Bhat GS, Shetty A, Hegde MN, Shetty P. The, "butterfly effect" and its correlation to the direction of the fracture line in root dentin. J Endod. 2021;47(5):787–92.